eNeuro

Research Article: New Research | Development

NGF- and BDNF-dependent DRG sensory neurons deploy distinct degenerative signaling mechanisms

https://doi.org/10.1523/ENEURO.0277-20.2020

Cite as: eNeuro 2020; 10.1523/ENEURO.0277-20.2020

Received: 19 June 2020
Revised: 3 December 2020
Accepted: 7 December 2020

Title:

NGF- and BDNF-dependent DRG sensory neurons deploy distinct degenerative signaling mechanisms

Abbreviated Title: Mechanisms of BDNF withdrawal-induced degeneration

Authors:

Andrés de León[1,2], Julien Gibon[2], Philip A. Barker[2]

[1]Department of Neurology and Neurosurgery, Montreal Neurological Institute, McGill University, Montreal, Quebec H3A 2B4, Canada; [2]Department of Biology, University of British Columbia Okanagan, Kelowna, British Columbia V1V 1V7, Canada.

Author Contributions:
ADL: Designed Research, performed research, Analyzed data and, Wrote the paper
JG and PAB: Designed Research, Analyzed data and, Wrote the paper

Correspondence should be addressed to: Philip Barker at: philip.barker@ubc.ca
Number of figure: 10
Number of Tables: 0
Number of Multimedia: 0
Number of words for Abstract: 186
Number of words for significance statement: 101
Number of words for introduction: 770
Number of words for discussion: 1455

Conflict of Interest: Authors report no conflict of interest

Funding sources: *This work was supported by Canadian Institute of Health Research to Philip Amos Barker (Grant MOP137057).*

NGF- and BDNF-dependent DRG sensory neurons deploy distinct degenerative signaling mechanisms

Andrés de León[1,2], Julien Gibon[2], Philip A. Barker[2]

[1]Department of Neurology and Neurosurgery, Montreal Neurological Institute, McGill University, Montreal, Quebec H3A 2B4, Canada; [2]Department of Biology, University of British Columbia Okanagan, Kelowna, British Columbia V1V 1V7, Canada.

This work was supported by Canadian Institute of Health Research to Philip Amos Barker (Grant MOP137057).

Abstract

The nerve growth factor (NGF) and brain-derived neurotrophic factor (BDNF) are trophic factors required by distinct population of sensory neurons during development of the nervous system. Neurons that fail to receive appropriate trophic support are lost during this period of naturally occurring cell death. In the last decade, our understanding of the signalling pathways regulating neuronal death following NGF deprivation has advanced substantially. However, the signaling mechanisms promoting BDNF-deprivation induced sensory neuron degeneration are largely unknown. Using a well-established *in vitro* culture model of dorsal root ganglion (DRG), we have examined degeneration mechanisms triggered upon BDNF withdrawal in sensory neurons. Our results indicate differences and similarities between the molecular signalling pathways behind NGF and BDNF deprivation-induced death. For instance, we observed that the inhibition of Trk receptors (K252a), PKC (Gö6976), protein translation (cycloheximide) or caspases (zVAD-fmk) provides protection from NGF deprivation-induced death but not from degeneration evoked by BDNF-withdrawal. Interestingly, degeneration of BDNF-dependent sensory neurons requires BAX and appears to rely on reactive oxygen species generation rather than caspases to induce degeneration. These results highlight the complexity and divergence of mechanisms regulating developmental sensory neuron death.

Significant statement

The elimination of neuronal cells generated in excess during embryonic stages characterizes the maturation of the nervous system. Here we address the developmental cell death mechanisms of BDNF-dependent dorsal root ganglion neurons *in vitro*, comparing and contrast them with those deployed in NGF-dependent sensory neurons. We observe several important differences between the molecular signalling pathways behind NGF and BDNF deprivation-induced death. Significantly, degeneration of BDNF-dependent sensory neurons requires BAX but not caspase activation, instead reactive oxygen species generation appears to play a key role in degeneration. This work highlights the complexity of cell death mechanisms in distinct embryonic sensory neuron populations.

Introduction

The developing nervous system undergoes a period of neuronal cell death during embryogenesis (Patel et al., 2000, Buss et al., 2006, Schuldiner and Yaron, 2015). In this period, neurons that fail to receive trophic support die by apoptosis (Burek and Oppenheim, 1996), a type of cell death also commonly observed in neurodegenerative diseases (Kirkland and Franklin, 2003, Fischer and Glass, 2007, Saxena and Caroni, 2007, Vickers et al., 2009, Tait and Green, 2010, Kanaan et al., 2013). The mammalian peripheral nervous system (PNS) offers a well-characterized context to study developmental neuronal apoptosis. Diverse sub-types of sympathetic and sensory neurons develop, compete, survive or die based on their capacity to bind enough trophic support from their target tissue (Barde, 1989, Saxena and Caroni, 2007).

Neurotrophins are crucial regulators of survival during the development of the nervous system. Alterations of their levels induce dramatic changes of innervation in the adult PNS (Levi-Montalcini and Booker, 1960, Ernfors et al., 1994a, Ernfors et al., 1994b, Tessarollo et al., 1997). In mammals, the neurotrophin family is composed of the nerve growth factor (NGF), brain-derived neurotrophic factor (BDNF), neurotrophin-3 (NT3) and neurotrophin-4/5 (NT4/5). With equal low affinity and no selectivity, each neurotrophins can bind to the pan-neurotrophin receptor p75 (p75NTR), and with high affinity to the tropomyosin-related kinase (Trk) receptor family: with NGF binding to TrkA, BDNF and NT4/5 to TrkB and NT3 to TrkC. Sympathetic and sensory neurons can be classified based on their expression profile of Trk receptors and their requirement for neurotrophins. Most sympathetic and sensory neurons depend on the NGF-TrkA signaling pathway during development (Kirstein and Fariñas, 2002, Glebova and Ginty, 2005, Lallemend and Ernfors, 2012). *In vitro* models using cultured sympathetic and dorsal root ganglia (DRG) neurons that are maintained and then withdrawn from NGF have provided many key insights into the cell autonomous mechanisms that drive developmental neuronal cell death (Unsain et al., 2013, Unsain et al., 2014, Geden et al., 2019). Recent work has shown that embryonic sensory neurons deprived of NGF results in PKC activation, ROS production, and TRPV1 activation which in turn induces a large increase in axoplasmic Ca^{2+} required for degeneration (Johnstone et al., 2018, Johnstone et al., 2019). To date, almost all

studies have focused on NGF sensitive peripheral neurons and mechanisms driving developmental neuronal death in other peripheral neuronal populations remains essentially unknown. In the present study, we asked whether the degenerative cascade initiated by NGF withdrawal could be extrapolated to population of neurons dependent on other neurotrophins, with a particular focus on the degenerative processes affecting BDNF-sensitive neurons.

Here, we show that NGF- and BDNF-dependent DRG neurons undergo axonal blebbing, reduced axonal area, increased extracellular phosphatidylserine, and rise in intracellular Ca^{2+} when withdrawn from trophic support. Further, degeneration of both classes of neurons require the pro-apoptotic protein BAX. However, unlike NGF-sensitive neurons, degeneration of BDNF-dependent deprivation does not require Trk activity, PKC activity or caspase activity and instead requires reactive oxygen species (ROS). Together, these results highlight the complexity and divergence of the mechanisms underlying trophic factor deprivation-induced neuronal cell death during development in the PNS.

Materials and Methods

Mouse strains

CD1 mice were purchased from Charles River Laboratories (Montreal, Canada). The previously described p75NTR knockout mice (Lee et al., 1992) and BAX knockout mice (Knudson et al., 1995) were maintained in a C57Bl6 strain background. Animal procedures and experiments were approved by the University of British Columbia animal care committee and the Canadian Council of Animal Care. Efforts were made to reduce animal handling and use.

Culturing and trophic factor deprivation of DRG explants

Dorsal root ganglia (DRG) were dissected from E13.5 mouse embryos and seeded in 12-well plastic (Grenier) or 4-well glass-bottom dishes (CellVis) sequentially coated with 1 mg/ml poly-D-lysine (Sigma-Aldrich), 10 µg/ml laminin-entactin complex (Corning) and 0.1 mg/ml PurCol bovine collagen (Advanced Biomatrix). Explants were grown in phenol-red Neurobasal media (Invitrogen) supplemented with 2% B27 serum-free supplement (Invitrogen), 1% L-glutamine (Wisent), 1% penicillin/streptomycin (Wisent), 10 µM 5-fluoro-2'-deoxyuridine (FDU, Sigma-Aldrich) and 12.5 ng/ml NGF (CedarLane) or 37.5 ng/ml BDNF (CedarLane) at 37ºC, 5% CO_2. Deprivation of neurotrophic support was accomplished using 2.0 µg/ml of function blocking antibodies against NGF (homemade rabbit polyclonal antibody raised against 2.5s NGF; (Acheson et al., 1991)) or BDNF (mouse monoclonal, DSHB #9-b) in complete fresh media without neurotrophic supplementation.

βIII-tubulin immunocytochemistry, imaging and quantification of axon degeneration

DRG explants were fixed in 4% paraformaldehyde solution in phosphate saline buffer (PBS) for 15 minutes, washed once in PBS and blocked in 5% milk in Tris-Borate buffer and 0.3% Triton-X100 for one hour at room temperature (RT). Explants were incubated overnight at 4ºC with mouse monoclonal antibody against βIII-tubulin (Millipore, MAB5564) diluted 1:10000 in blocking solution. DRGs were washed twice in PBS and then incubated with goat anti-mouse conjugated to Alexa Fluor 488 (Jackson ImmunoResearch, 115-545-003) diluted 1:5000 in blocking solution for a minimum of 3

hours at RT. Explants were imaged using a Zeiss ObserverZ.1 inverted epifluorescence microscope with an automated motorized stage (5x magnification with tilling). From a stitched master image of the plate generated by Zen 2 software (Zeiss, Canada), quarter DRG fields were cropped to generate a set of images for analysis using the R script program Axoquant 2.0 (Johnstone et al., 2018). Final measurements were plotted as the mean axonal area of DRGs from three embryos. Increments of 500 µm were used for statistical analysis (normalized to same increments in control condition).

Assessment of DRG explant survival with live Calcein-AM staining

DRG explants were treated with 1 µg/ml Calcein-AM (AAT Bioquest) in neurobasal media for 1 hour at 37ºC then switched to clear HBSS-based complete media supplemented with HEPES to maintain physiological pH. Explants were tiled-imaged using a Zeiss ObserverZ.1 inverted epifluorescence microscope with an automated motorized stage. From a stitched master image of the plate generated by the Zen 2 software, cell bodies and Schwann cells were cropped out and a binary mask image of each explants was created using NIH Image J software. Explant area and mean pixel intensity value corrected by the background signal were quantified to provide either the area of Calcein-AM-stained axons over a specified threshold or Calcein-AM fluorescence intensity per unit of area. DRG explants from the same embryo were pooled and averaged to generate the mean value for each embryo. Measurements were normalized relative to NGF or BDNF wild-type conditions.

Annexin-V staining, imaging and quantification

DRG explants seeded on glass bottom dishes (CellVis) were incubated with 1 µg/ml Annexin-V (AAT Bioquest) in annexin-V buffer (10 mM HEPES/NaOH, pH7.4, 140 mM NaCl, 2.5 mM $CaCl_2$) for 15 min at room temperature. DRGs were washed and tiled-imaged in the annexin-V buffer using a Zeiss Observer Z.1 inverted epifluorescence microscope (40x magnification). Stitched master images of each explant generated by Zen 2 software were cropped to eliminate soma and Schwann-cell area and axonal annexin-V area was measured using a binary mask over an established threshold for all explants. DRG explants from the same embryo were pooled

and averaged to generate the mean value for each embryo. Measurements were normalized relative to NGF or BDNF controls.

Ca^{2+} imaging with Fluo-4 and quantification

DRG explants were seeded on glass bottom dishes (CellVis) and treated with 5 µM Fluo-4 AM (Invitrogen) in neurobasal media for 15 min at 37ºC, washed with HBSS and switched to clear HBSS-based complete media supplemented with HEPES (final concentration 20 mM) to maintain its physiological pH. Explants were tiled-imaged using a Zeiss ObserverZ.1 inverted epifluorescence microscope with an automated motorized stage at 40x magnification. Employing NIH Image J software, stitched master images of each explant were cropped to eliminated soma and Schwann-cell area. From there, a binary mask image of remaining axons was created to measure area and mean pixel intensity corrected by background signal. After calculating the intensity per unit of axonal area, DRG explants from the same embryo were pooled and averaged to generate the mean value per embryo. Measurements were normalized and expressed as fold-change from NGF or BDNF controls.

Immunoblotting

For SDS-PAGE and western-blot analysis, a total of 25 DRG explants per well were seeded in 12-well plastic plates (Grenier). For protein harvesting, cultures were washed with PBS, and DRGs were scraped into 90 µl of sample buffer (4% SDS, 20% glycerol, 10% 2-mercaptoethanol, 0.004% bromophenol blue and 0.125 M Tris-HCl, pH approx. 6.8). Samples were boiled for five minutes, centrifuged and stored at -80ºC for later analysis. Antibodies used for immunoblotting were: anti-βIII-tubulin (Millipore MAB5564, 1:10000), anti-neurofilament M (Millipore AB1987, 1:1000), anti-caspase-3 (NEB 9662, 1:1000), anti-TrkA (Millipore 06-574, 1:1000), anti-TrkB (Millipore 07-225, 1:1000), anti-TrkC (Millipore 07-226, 1:1000) and the previously described anti-p75NTR (Barker and Shooter, 1994).

Pharmacological PKC, Trk, caspase, autophagy, translation and necroptosis inhibitors

Stocks of PKC inhibitor Gö6976 (10 mM, Tocris 2253, UK), Trk receptor inhibitor K252a (200 µM, Calbiochem #420298, Israel), pan-caspase inhibitors Boc-D-fmk (10 mM, Abcam ab142036, USA), zVAD-fmk (20 mM, R&D systems FMK001, USA), and necroptosis inhibitor necrostatin-1 (NEC-1, 100 mM, Sigma-Aldrich N9037, USA) were prepared in dimethylsulphoxide (DMSO) and used at 1:1000 dilution (final concentration of DMSO below 0.1%). The translation inhibitor cycloheximide (CHX, R&D systems 0970/100, USA) was dissolved at 1.0 g/L in water and used at 1:1000. Autophagy inhibitor 3-methyladenine (3MA, Sigma-Aldrich M9281, Israel) was dissolved at 10 mM in phenol-red neurobasal media. Drugs were applied at the same time that the trophic factor withdrawal was initiated.

EGTA, NAC and NAD+ preparation

Ethylene glycol-bis (β-aminoethyl ether)-N,N,N′,N′-tetraacetic acid (EGTA, AlfaAesar A16086, UK, final concentration 5 mM), N-acetylcysteine (NAC, Sigma, A9165, China, final concentration 20 mM) or nicotinamide adenine dinucleotide (NAD+, Sigma-Aldrich, N7004, USA, final concentration 5 mM) were dissolved in Neurobasal media, pH adjusted to 7.4 and filtered by 0.22 µm for final treatment of DRG explants. After 48 hours of growth in NGF or BDNF, cultures were either maintained with trophic support or deprived of it, in the absence or presence of each specific compound for the entire deprivation period.

Experimental design and statistical analysis

Data were plotted and analyzed using Prism 6 (Graph-Pad). All data were presented as mean ±SEM. The number of embryos *n* in each experiment or condition is described in each figure legend. Mann-Whitney test (unpaired, two-tailed) was used for two-group experiments comparisons. Two-way ANOVA with Bonferroni's *post hoc* test or Tukey's post hoc test was used to analyze differences in multiple groups. In all graphs, non-significant ($p>0.05$): ns, * (or other symbols) $p<0.05$, **$p<0.01$, ***$p<0.001$ and ****$p<0.0001$.

Results

The apoptotic machinery involved in NGF deprivation-induced axonal degeneration in DRG neurons is well-characterized (Geden et al., 2019). However, our knowledge of axonal degeneration induced by BDNF deprivation is rudimentary. To begin to address this, we characterized BDNF withdrawal-induced axon degeneration in DRG neurons generated from E13.5 mice embryos. Figure 1A shows that E13.5 DRGs cultured in the presence of BDNF survived and developed neurites (quantified in 1B). The extent and density of neurites was maximal at a BDNF concentration of 125 ng/ml (Figure 2A) but even at this concentration, processes were significantly less dense and shorter than within parallel DRGs cultured in NGF (data not shown). It was also noted that DRGs derived from the lumbar and cervical parts of the spinal cord extended more exuberant processes in response to BDNF than DRGs derived from the thoracic region (Figure 2B). For subsequent experiments, cervical DRG neurons were routinely cultured using 37.5 ng/ml of BDNF or 12.5 ng/ml of NGF. For BDNF-deprivation studies, cells were grown in BDNF for 48 hours and then switched to BDNF-free media supplemented with an anti-BDNF monoclonal antibody for 24 hours. Axons maintained and then deprived of BDNF in this manner showed morphological signs of degeneration and blebbing (Figure 1C higher magnification, quantified in 1D).

Cell biological and biochemical indications of BDNF-withdrawal induced axonal degeneration were also established. DRG axons that were maintained and then deprived of either NGF or BDNF show a significant increase of extracellular phosphatidylserine, determined using Annexin-V staining, and a drastic decrease of viable axons, determined using Calcein-AM (Figure 3A, quantified in 3B). It has been previously shown that NGF deprivation induces a large increase in axoplasmic Ca^{2+} ~15 hours after deprivation (Johnstone et al., 2018, Johnstone et al., 2019) and here show that BDNF-withdrawal induces a similar elevation in axonal Ca^{2+} 15 hours after trophic deprivation (Figure 3C, quantified in 3D).

To characterize the neurotrophin receptor complement in DRG explants, protein lysates from E13.5 DRGs maintained in NGF or BDNF for 72 hours were analyzed by immunoblot. DRGs cultured in NGF expressed abundant TrkA, TrkB, and p75NTR but

low amounts of TrkC. In contrast, DRG neurons cultured in BDNF expressed abundant TrkB, TrkC and p75NTR (Figure 4A) but essentially no TrkA.

Previous studies have indicated that p75NTR is required for cell death of sympathetic neurons during development (Deppmann et al., 2008) but not for apoptosis of DRG sensory neurons. p75NTR has also been shown to be required for sympathetic neuron axon degeneration (Bamji et al., 1998, Singh et al., 2008). To determine if p75NTR is required for axonal loss after NGF or BDNF deprivation in DRG axons, we assessed axonal loss in DRGs from p75NTR-null embryos (Figure 4B). When maintained and then withdrawn from NGF or BDNF, the degree of axonal degeneration was the same in wild-type and p75NTR-null DRGs (Figure 4C), ruling out a direct role for p75NTR in axon loss induced by neurotrophin withdrawal.

TrkA and TrkC have been implicated as dependence receptors (Nikoletopoulou et al., 2010) and recent studies have suggested that NGF deprivation activates a TrkA-dependent apoptotic signalling pathway (Feinberg et al., 2017). Consistent with this, Figure 4D and E show that a low concentration of the pan-Trk inhibitor K252a (200 nM) rescues NGF-deprivation induced axon degeneration of DRG sensory neurons but has no effect on BDNF deprivation-induced DRG axon degeneration (Figure 4D, quantified in 4E). These results are consistent with previous findings showing that TrkB does not have dependence receptor activity (Nikoletopoulou et al., 2010).

To begin to discern signaling mechanisms driving BDNF deprivation-induced axon loss, we tested several compounds known to inhibit NGF withdrawal-induced axon degeneration or to inhibit neuronal cell death. PKC inhibitor Gö6976 rescues NGF deprivation-induced apoptosis (Johnstone et al., 2019) but had no effect on BDNF deprivation (Figure 5A, quantified in 5B). Likewise, the Ca^{2+} chelator EGTA is a potent inhibitor of axon loss induced by NGF withdrawal in DRG neurons (Johnstone et al., 2018) but did not protect against BDNF deprivation (Figure 5C, quantified in 5D). The translation inhibitor cycloheximide (CHX) also significantly protects axons from degeneration induced by NGF deprivation (Figure 6A) but has no effect on axon degeneration induced by BDNF withdrawal. Finally, neither the autophagy inhibitor 3-methyladenine (3-MA), the necroptosis inhibitor necrostatin-1 (NEC-1) nor nicotinamide

adenine dinucleotide (NAD+) blocked BDNF withdrawal-induced axonal degeneration of DRG sensory neurons (Figure 6B, C and D).

BAX is a central player in neuronal apoptosis and crucial for NGF-deprivation induced axonal degeneration (Patel et al., 2000, Schoenmann et al., 2010, Simon et al., 2012). To address the role of BAX in BDNF-deprived DRG sensory neurons, BAX-null DRG neurons were maintained in NGF or BDNF and then deprived of trophic support. Figure 7 shows that axons lacking BAX were significantly protected from degeneration induced by NGF- and BDNF-deprivation (Figure 7A, quantified in 7B).

Caspase-3 is crucial for NGF deprivation-induced axonal degeneration (Simon et al., 2012, Unsain et al., 2013) and the requirement for BAX in BDNF withdrawal-induced axonal loss suggests that caspases may also play a role in axonal degeneration induced by BDNF deprivation. However, Figure 8A shows that while caspase inhibition efficiently rescued axons from NGF deprivation, two distinct pan-caspase inhibitors (Boc-D-fmk and zVAD-fmk) did not reduce axonal degeneration in neurons that were maintained and then withdrawn from BDNF (Figure 8A, quantified in 8B and Figure 9A, quantified in 9B). Correspondingly, NGF deprivation decreased levels of pro-caspase-3 and increased cleaved caspase-3 whereas levels of pro- and cleaved caspase-3 did not change in neurons maintained and then withdrawn from BDNF for 15, 24 and 30 hours (Figure 9C and data not shown). Taken together, these results indicate that BAX activity mediates BDNF deprivation-induced axonal degeneration through a caspase-independent pathway.

Several reports have shown that BAX can facilitate production of mitochondrial reactive oxygen species (Kirkland and Franklin, 2001, Kirkland et al., 2002, Kirkland and Franklin, 2007, Kirkland et al., 2010). To explore whether ROS play a role in neurotrophin deprivation-induced axonal degeneration, axons maintained in NGF or BDNF were exposed to N-acetylcysteine (NAC), a ROS scavenger, and then withdrawn from trophic support. Figure 10 shows that axonal degeneration induced by either NGF or BDNF deprivation was blocked in the presence of NAC, indicating that ROS are required for axonal degeneration induced by neurotrophin deprivation.

Discussion

The mammalian peripheral nervous system has proven a useful system for identifying specific mechanisms that are required for developmental neuronal degeneration. Substantial understanding of processes that mediate neuronal cell death and axonal destruction has been obtained from analyses of NGF-dependent DRG neurons maintained *in vitro*. However, less is known about signaling pathways that lead to the developmental loss of other sensory neuron populations. In this study, we have examined mechanisms that promote the developmental degeneration of BDNF-dependent sensory neurons. Our observations show that BDNF-dependent DRG sensory neurons employ destructive mechanisms distinct from those employed by NGF-dependent sensory neurons.

Growth differences in NGF- and BDNF-dependent DRG populations. Several studies point to BDNF as a key trophic factor required to sustain the survival of different neuronal populations *in vivo* and *in vitro* (Johnson et al., 1986, Kalcheim et al., 1987, Liebl et al., 1997). Cranial sensory neurons are highly dependent on BDNF for survival and growth (Hellard et al., 2004) whereas only a subpopulation of DRG sensory neurons requires BDNF for survival during development (Huber et al., 2000, Valdés-Sánchez et al., 2010). Here we showed that BDNF supports the survival and growth of neurons within E13.5 DRG explants, with neurite length steadily increasing with the time of trophic factor exposure. However, BDNF-dependent outgrowth was considerably less than that supported by NGF, consistent with the observation that only 8% of DRG neurons are TrkB+ while 80% are TrkA+ (Fariñas et al., 1998, Ernsberger, 2009). Thus, in the absence of NGF, the vast majority of DRG sensory neurons degenerate, leaving behind a small number of TrkB+ neurons. The reduced capacity of BDNF to promote neurite extension in culture may also reflect the fact that TrkB, but not TrkA, is down-regulated after exposure and binding to its ligand (Sommerfeld et al., 2000, Haapasalo et al., 2002) and that BDNF activates Ras considerably less effectively than NGF (Borasio et al., 1989, Carter et al., 1995).

Trophic deprivation-induced degeneration of BDNF-dependent DRG sensory neurons. To mimic BDNF deprivation that occurs during embryonic development, E13.5 DRGs were maintained in BDNF and then withdrawn from the factor. A function blocking monoclonal antibody directed against BDNF was deployed to inactivate any residual BDNF remaining. BDNF deprivation resulted in neurite blebbing, a hallmark morphology of degenerating neurites, and caused a significant reduction of area occupied by neurites. Axonal degeneration provoked by BDNF deprivation was confirmed using the live dye Calcein-AM and by staining with Annexin-V, which detects phosphatidylserine on the outer leaflet of the plasma membrane, a prototypical signal driving phagocytosis of cells undergoing cell death (Wakatsuki and Araki, 2017, Shacham-Silverberg et al., 2018). Calcein-AM is a sensitive staining technique to quantify axonal integrity. However, Calcein-AM binds calcium after being hydrolyzed by intracellular esterase and its use was not compatible with some of our treatments (e.g. EGTA). Therefore, Calcein-AM staining was used to follow the effect of p75NTR or BAX deficiency on axonal integrity during trophic deprivation conditions and the effects of drugs on axonal degeneration was studied based on βIII-tubulin staining and quantified with Axoquant 2.0 (as described in Johnstone et al., 2018).

How does BDNF deprivation trigger degeneration in BDNF-dependent sensory neurons? Several studies have indicated that unliganded TrkA promotes pro-apoptotic signaling in sympathetic and sensory neurons withdrawn from NGF (Tauszig-Delamasure et al., 2007, Nikoletopoulou et al., 2010, Feinberg et al., 2017). In this sense, TrkA can be considered a ‘dependence receptor’ that promotes survival signaling when bound by ligand but drives death signaling upon ligand withdrawal (Nikoletopoulou et al., 2010). Here we showed that the pan-Trk kinase inhibitor K252a prevented degeneration normally induced by NGF deprivation but had no effect on degeneration induced by BDNF deprivation, indicating that TrkA, but not TrkB, behaves as a dependence receptor. This finding agrees with those of Barde’s group who found that TrkA and TrkC behave as dependence receptors but the BDNF receptor TrkB is incapable of doing so (Nikoletopoulou et al., 2010).

We also questioned the role of p75NTR in BDNF-deprivation. Depending on the cellular and molecular context, the low-affinity neurotrophin receptor can drive pro-survival or pro-death signaling (Roux and Barker, 2002, Mehlen and Bredesen, 2004). Although p75NTR is crucial for sympathetic neuronal remodeling during embryonic development (Bamji et al., 1998, Singh et al., 2008), here we found that p75NTR had no effect on degeneration of sensory neurons maintained and then withdrawn from either NGF or BDNF.

PKC plays an indispensable role in DRG degeneration induced by NGF withdrawal (Johnstone et al., 2019) but PKC inhibitors had no effect on BDNF-withdrawal induced degeneration. Likewise, cycloheximide, a potent blocker of NGF-withdrawal induced degeneration had no effect on BDNF-withdrawal induced deprivation. Therefore, degeneration mechanisms of sensory neurons maintained and then withdrawn from BDNF are fundamentally distinct from those in NGF-dependent sensory neurons.

Role of Ca^{2+} in BDNF deprivation induced degeneration of BDNF-dependent DRG sensory neurons. In NGF-dependent DRG neurons, extracellular Ca^{2+} chelation blocks both the axoplasmic Ca^{2+} rise and the subsequent degenerative process that normally occur upon NGF withdrawal (Johnstone et al., 2018, Johnstone et al., 2019). Here we showed that BDNF deprivation induces Ca^{2+} rise in neurites of BDNF-dependent DRG explants yet Ca^{2+} chelation with EGTA did not rescue BDNF-deprivation induced degeneration. We observed that Ca^{2+} chelation in non-deprived DRG explants induced growth arrest and previous work has established that the ability of BDNF to sustain neuronal survival is reduced in comparison to NGF (Borasio et al., 1989, Carter et al., 1995). These results suggest a delicate homeostasis within BDNF-dependent DRG neurons. The lack of Ca^{2+} paired with the trophic support deprivation could - in these sensitive cells - favor degeneration instead of protection. Therefore, our results do not completely rule out an active role of Ca^{2+} in the degenerative mechanism of BDNF-deprived DRG neurons.

ROS play a central role in the degeneration induced by BDNF deprivation. ROS were initially described solely as toxic cellular by-products, but a growing body of evidence

has established ROS as endogenous modulators of numerous physiological functions (Wilson et al., 2018). A recent study showed that NGF deprivation in sensory neurons induces ROS production through a PKC/NOX pathway and that ROS scavengers rescue degeneration of NGF-dependent sensory neurons after trophic deprivation (Johnstone et al., 2019). In the present work we showed that the antioxidant NAC partially protects DRG neurons from BDNF-deprivation, suggesting that ROS play a role in the degeneration of BDNF-dependent sensory neurons. However, blocking PKC during BDNF deprivation had no effect on degeneration, indicating that the contribution of NOX-derived ROS to BDNF degeneration pathway is likely minor. Consistent with this, we found that NOX inhibitors that block NGF-withdrawal induced degeneration had no effect on BDNF-withdrawal-induced degeneration (data not shown).

Aside from NOX complexes, the other major source of ROS in the cell is mitochondria. Our results show that BAX is required for BDNF-deprivation induced degeneration of DRG neurons *in vitro*, consistent with *in vivo* data showing the importance of BAX during developmental cell death of BDNF-dependent cranial sensory neurons, particularly from nodose, petrosal and vestibular ganglia (Hellard et al., 2004). BAX translocates to the mitochondria and induces mitochondria outer membrane permeabilization (MOMP) (Kalkavan and Green, 2018); in many circumstances MOMP provokes the release of the pro-apoptotic proteins SMAC and cytochrome *c*, engaging in the recruitment and activation of executioner caspases. However, since cleaved caspase-3 levels did not rise - and caspase blockers did not slow neuronal loss - in DRG sensory neurons deprived of BDNF, BAX must facilitate cell loss through a caspase-independent mechanism in this setting. BAX-dependent and caspase-independent cell death typically involves mitochondrial potential loss and failure (Deshmukh et al., 2000, Chang and Johnson, 2002, Chang et al., 2003, Lang-Rollin et al., 2003), with BAX-mediated MOMP inducing an increase of mitochondrial ROS production (Jiang et al., 2008, Garcia-Perez et al., 2012). In some circumstances, BAX-mediated MOMP and ROS production can trigger the formation of the mitochondria permeability transition pore which has been implicated in several forms of neuronal death (Lamarche et al., 2013).

A recent review by Fricker et al. (2018) proposed the existence of at least twelve different cell death pathways, highlighting the diversity and complexity of cellular death mechanisms (Fricker et al., 2018). Here, we examined pro-degenerative pathways such as necroptosis and autophagy and mechanisms such as protein translation and NAD+ metabolism. Our results showed that several of these pathways impinge on the degenerative process induced by NGF deprivation but blockade of necroptosis, autophagy or translation nor NAD+ supplementation rescued degeneration evoked by BDNF withdrawal.

In conclusion, we have provided the first in depth characterization of the mechanisms that mediate degeneration of BDNF-dependent DRG sensory neurons upon trophic factor withdrawal. We show that the pathways regulating the degeneration of BDNF-dependent DRG sensory neurons requires BAX and ROS but are Trk- and caspase-independent and distinct from those invoked upon NGF-withdrawal.

Figure Legends

Figure 1. Comparative growth of NGF- and BDNF-dependent DRG sensory neurons and their degeneration induced by trophic factor withdrawal. A) βIII-tubulin staining of embryonic mice DRG explants cultured in the presence of NGF (12.5 ng/ml) or BDNF (37.5 ng/ml) for 48, 72 or 120 hours (Scale bar = 1000 µm). B) Quantification of axonal area as a function of the distance from the soma using Axoquant 2.0 (Johnstone et al., 2018) and plotted in 500-µm bins. The difference between the relative axonal area between NGF-dependent and BDNF-dependent DRG growth at different time points were analyzed by two-factor ANOVA and Bonferroni's *post hoc* comparison and plotted with mean and SEM (n = 3 embryos for each condition; data shown is representative of 3 independent experiments); (*) NGF vs. BDNF; ***p < 0.001, ****p < 0.0001. C) DRG explants cultured in the presence of NGF or BDNF for 48 hours and then either maintained with trophic support or deprived with a function blocking anti-NGF (2 µg/ml) or anti-BDNF (2 µg/ml) for the following 24 hours, before fixation and immunostaining with βIII-tubulin (Scale bar = 1000 µm). D) NGF and BDNF deprivation for 24 hours results in a significant loss of βIII-tubulin-stained axons expressed as axonal area relative to 0-500 µm NGF or BDNF controls; analyzed by two-factor ANOVA and Bonferroni's *post hoc* comparison and plotted with mean and SEM. **p < 0.01, ***p < 0.001, ****p < 0.0001.

Figure 2. Axon growth of BDNF-dependent DRGs from the cervical, the thoracic or the lumbar region of the spinal cord with several concentration of BDNF. A) Calcein-AM stained DRGs from cervical, thoracic or lumbar spinal cord segments of E13.5 mice embryos were grown for 48 hours in 0, 12.5 or 125 ng/ml of BDNF (Scale bar = 500 µm). B) Quantification of Calcein-AM stained axonal area relative to Calcein-AM stained axonal area of lumbar DRGs at 125 ng/ml analyzed by one-factor ANOVA and Tukey's *post hoc* comparison and plotted with mean and SEM (n = 3 embryos for each condition; data shown is representative of 3 independent experiments). ns: non-significant, *p < 0.05.

Figure 3. DRG sensory neurons undergoing BDNF deprivation display increased extracellular phosphatidylserine and increased axoplasmic Ca^{2+}. A) DRG explants cultured in the presence of NGF or BDNF for 48 hours and then either maintained with trophic support or deprived with an antibody against NGF or BDNF for the following 24 hours were co-stained with Calcein-AM (green) and Annexin-V (red) to measure the area of healthy axons versus axons displaying phosphatidylserine, an apoptotic marker, respectively (NGF scale bar = 1000 μm, merge scale bar = 50 μm; BDNF scale bar = 500 μm, merge scale bar = 50 μm). B) Both NGF and BDNF-deprivation induced a significant decrease in Calcein-AM positive axonal area (n = 5 embryos in NGF and n = 8 embryos in BDNF from pooled litters) and a significant increase in Annexin-V area (n = 5 embryos in NGF dep. 24h and n = 10 embryos in BDNF dep. 24h from pooled litters). The bar plots show mean, min/max and 25/75% for each panel, analyzed by two-tailed Mann-Whitney tests with *p < 0.05, **p < 0.01, ***p < 0.001. C) DRG explants cultured in NGF or BDNF were maintained in trophic media or withdrawn from trophic support for 15 hours before staining with Fluo-4 and imaged by epifluorescence microscopy (NGF scale bar = 1000 μm; BDNF scale bar = 200 μm). D) Both NGF and BDNF deprivation induced a significant increase in axonal Fluo-4 intensity (n = 4 embryos in NGF and n = 6 embryos in BDNF from pooled litters). The bar plots show mean, min/max and 25/75% for each panel, analyzed by two-tailed Mann-Whitney tests with *p < 0.05.

Figure 4. Trk receptor inhibition protects axons from NGF deprivation but not from BDNF-deprivation whereas p75NTR deficiency confers no protection to axons established in NGF or BDNF. A) Protein lysates collected from E13.5 DRG explants cultured in the presence of NGF (12.5 ng/ml) or BDNF (37.5 ng/ml) for 48 hours were analyzed by immunoblot against TrkA, TrkB, TrkC, p75NTR and, βIII-tubulin. B) p75NTR knock-out does not rescue axons from degeneration after NGF or BDNF withdrawal. DRG explants from mixed-genotyped E13.5 litters were cultured in the presence of NGF or BDNF for 48 hours and then either maintained or withdrawal from trophic support for 24 hours before being lived stained with Calcein-AM (NGF scale bar = 1000 μm; BDNF scale bar = 500 μm). C) Quantification of Calcein-AM intensity

normalized by axonal area and relative to wild-type control. Non-significant difference was observed between wild-type and p75NTR-null DRG explants deprived of NGF or BDNF (n = 4 embryos in NGF and n = 4 embryos in BDNF from pooled litters). Analyzed by two-way ANOVA and Tukey's *post hoc* comparison and plotted with median and SEM. *p < 0.05, **p < 0.01, ***p < 0.001, ****p < 0.0001. D) DRG explants cultured in NGF or BDNF were either maintained in trophic media or withdrawn from trophic support with or without the Trk inhibitor K252a (200 nM) for 24 hours before fixing, immunostaining for βIII-tubulin and imaged by epifluorescence microscopy (NGF scale bar = 1000 μm; BDNF scale bar = 500 μm). E) K252a rescued degeneration induced by NGF deprivation but not by BDNF deprivation. Quantification of axonal area as a function of the distance from the soma using Axoquant 2.0 and plotted in 500-μm binned segments relative to 0-500 μm NGF control (upper panel) or BDNF control (lower panel). The relative axonal area was analyzed by two-factor ANOVA followed by Tukey's *post hoc* comparison and plotted with mean and SEM (n = 3 embryos per condition for each condition; data shown is representative of 3 independent experiments); (∗) ctr. versus dep. 24h; (#) dep. 24h versus dep. 24h + K252a; ns: non-significant, **p < 0.01, ***p < 0.001, ****p < 0.0001.

Figure 5. PKC inhibitor Gö6976 and EGTA rescue degeneration induced by NGF deprivation but not BDNF deprivation. A) DRG explants cultured in NGF or BDNF were either maintained in trophic media or withdrawn from trophic support with or without PKC inhibitor Gö6976 (10 μM) for 24 hours before fixing, immunostaining for βIII-tubulin and imaged by epifluorescence microscopy (NGF scale bar = 1000 μm; BDNF scale bar = 500 μm). B) Quantification of axonal area as a function of the distance from the soma using Axoquant 2.0 (Johnstone et al., 2018) and plotted in 500-μm bins segments relative to 0-500 μm 48-hour time point. The relative axonal area was analyzed by two-factor ANOVA followed by Tukey's *post hoc* comparison and plotted with mean and SEM (n = 3 embryos per condition for each condition; data shown is representative of 3 independent experiments); (∗) control versus deprived 24h; (#) deprived 24h versus deprived 24h + Gö6976; ns: non-significant, *p < 0.05, ****p < 0.0001. C) DRG explants cultured in NGF or BDNF were either maintained in trophic media or withdrawn from

trophic support with or without Ca^{2+} chelator EGTA (5 mM) for 24 hours before fixing, immunostained for βIII-tubulin and imaged by epifluorescence microscopy (NGF scale bar = 1000 μm; BDNF scale bar = 500 μm). D) Quantification of axonal area as a function of the distance from the soma using Axoquant 2.0 and plotted in 500-μm binned segments. Ca^{2+} chelation rescued degeneration induced by NGF deprivation but not by BDNF deprivation. The relative axonal area was analyzed by two-factor ANOVA followed by Tukey's *post hoc* comparison and plotted with mean and SEM (n = 3 embryos per condition for each condition; data shown is representative of 3 independent experiments); (∗) ctr. versus dep. 24h; (#) dep. 24h versus dep. 24h + EGTA; ns: non-significant, ****p < 0.0001.

Figure 6. Translation, autophagy, necroptosis or Wallerian-like degeneration are not involved in BDNF deprivation-induced degeneration. A) DRG explants cultured in NGF or BDNF were maintained in trophic media or withdrawn from trophic support with or without translation inhibitor cycloheximide (CHX, 1 μg/ml) for 24 hours before fixing, immunostaining for βIII-tubulin and imaging by epifluorescence microscopy (NGF scale bar = 1000 μm; BDNF scale bar = 500 μm). Quantification of axonal area as a function of the distance from the soma plotted in 500-μm bins segments relative to 0-500 μm BDNF control. CHX rescued degeneration induced by NGF deprivation but not by BDNF deprivation. The relative axonal area was analyzed by two-factor ANOVA followed by Tukey's *post hoc* comparison and plotted with mean and SEM (n = 3 embryos per condition for each condition; data shown is representative of 3 independent experiments); (∗) ctr. versus dep. 24h; (#) dep. 24h versus dep. 24h + CHX; ns: non-significant, ****p < 0.0001. B) DRG explants were withdrawn from trophic support with or without the autophagy inhibitor 3-methyladedine (3-MA, 10 mM) for 24 hours before being immunostained for βIII-tubulin (NGF scale bar = 1000 μm; BDNF scale bar = 500 μm). Quantification of axonal area as a function of the distance from the soma plotted in 500-μm bins segments relative to 0-500 μm BDNF control. 3-MA rescued degeneration induced by NGF deprivation but not by BDNF deprivation. The relative axonal area was analyzed by two-factor ANOVA followed by Tukey's *post hoc* comparison and plotted with mean and SEM (n = 3 embryos per condition for each condition; data shown is

representative of 3 independent experiments); (∗) ctr. versus dep. 24h; (#) dep. 24h versus dep. 24h + 3-MA; ns: non-significant, *p < 0.05, **p < 0.01, ***p < 0.001, ****p < 0.0001. C) DRG explants were withdrawn from trophic support with or without the necroptosis inhibitor necrostatin-1 (NEC-1, 100 μM) for 24 hours before being immunostained for βIII-tubulin (NGF scale bar = 1000 μm; BDNF scale bar = 500 μm). Quantification of axonal area as a function of the distance from the soma plotted in 500-μm binned segments relative to 0-500 μm BDNF control. NEC-1 slightly rescued degeneration induced by NGF deprivation but not by BDNF deprivation. The relative axonal area was analyzed by two-factor ANOVA followed by Tukey's *post hoc* comparison and plotted with mean and SEM (n = 3 embryos per condition for each condition; representative of 3 independent experiments); (∗) ctr. versus dep. 24h; (#) dep. 24h versus dep. 24h + NEC-1; ns: non-significant, *p < 0.05, ***p < 0.001, ****p < 0.0001. D) DRG explants were withdrawn from trophic support with or without NAD+ (5 mM) for 24 hours before being immunostained for βIII-tubulin (NGF scale bar = 1000 μm; BDNF scale bar = 500 μm). Quantification of axonal area as a function of the distance from the soma plotted in 500-μm bins segments relative to 0-500 μm BDNF control. NAD+ rescued degeneration induced by NGF deprivation but not by BDNF deprivation. The relative axonal area was analyzed by two-factor ANOVA followed by Tukey's *post hoc* comparison and plotted with mean and SEM (n = 3 embryos per condition for each condition; data shown is representative of 3 independent experiments); (∗) ctr. versus dep. 24h; (#) dep. 24h versus dep. 24h + NAD+; ns: non-significant, *p < 0.05, **p < 0.01, ****p < 0.0001.

Figure 7. NGF and BDNF deprivation-induced degeneration require BAX. A) DRG explants from mixed-genotyped E13.5 litters were cultured in the presence of NGF or BDNF for 48 hours and then either maintained or withdrawn from trophic support for 24 hours before being lived stained with Calcein-AM (NGF scale bar = 1000 μm; BDNF scale bar = 500 μm). B) Quantification of Calcein-AM intensity normalized by axonal area and relative to wild-type control. A significant increase in Calcein-AM intensity was observed in both NGF or BDNF deprived BAX-null DRG explants compared with their deprived wild-type counterparts (n = 7 embryos in NGF/BDNF ctr., n = 5 embryos in

NGF/BDNF dep. 24h, from pooled litters). Data was analyzed by two-way ANOVA and Tukey's *post hoc* comparison and plotted with median and SEM. ns: non-significant, *p < 0.05, **p < 0.01, ****p < 0.0001.

Figure 8. pan-Caspase inhibition does not block degeneration induced by BDNF deprivation. A) DRG explants cultured in NGF or BDNF were maintained in trophic media or were withdrawn from trophic support with or without pan-caspase inhibitor Boc-D-fmk (10 μM) for 24 hours before fixing, immunostaining for βIII-tubulin and imaging by epifluorescence microscopy (NGF scale bar = 1000 μm; BDNF scale bar = 500 μm). B) Quantification of axonal area as a function of the distance from the soma was performed using Axoquant 2.0 (Johnstone et al., 2018) and plotted in 500-μm binned segments relative to 0-500 μm NGF/BDNF controls. Pan-caspase inhibitor Boc-D-fmk rescued degeneration induced by NGF deprivation but not by BDNF deprivation. The relative axonal area was analyzed by two-factor ANOVA followed by Tukey's *post hoc* comparison and plotted with mean and SEM (n = 3 for each condition; data shown is representative of 3 independent experiments); (∗) ctr. versus dep. 24h; (#) dep. 24h versus dep. 24h + Boc-D-fmk; ns: non-significant, ****p < 0.0001.

Figure 9. Cleaved form of executioner caspase-3 does not increase during BDNF deprivation. A) DRG explants cultured in NGF or BDNF were either maintained in trophic media or withdrawn from trophic support with or without pan-caspase inhibitor zVAD-fmk (20 μM) for 24 hours before fixing, immunostaining for βIII-tubulin and imaged by epifluorescence microscopy (BDNF scale bar = 1000 μm). B) Quantification of axonal area as a function of the distance from the soma plotted in 500-μm bins segments relative to 0-500 μm BDNF control. Pan-caspase inhibitor zVAD-fmk does not rescues degeneration induced by BDNF deprivation. The relative axonal area was analyzed by two-factor ANOVA followed by Tukey's *post hoc* comparison and plotted with mean and SEM (n = 3 embryos per condition for each condition; data shown is representative of 3 independent experiments); (∗) ctr. versus dep. 24h; (#) dep. 24h versus dep. 24h + zVAD-fmk; ns: non-significant, *p < 0.05, ***p < 0.001, ****p < 0.0001. C) Protein lysates collected from E13.5 DRG explants cultured in the presence

of NGF (12.5 ng/ml) or BDNF (37.5 ng/ml) for 48 hours were maintained or withdrawn from trophic support for 24 hours and then analyzed by immunoblot against Neurofilament-M (Nf-M) and caspase-3. Levels of Nf-M significantly deceased after either NGF and BDNF deprivation but only NGF deprived DRG lysates show a significant change in pro- and cleaved caspase-3 levels. Data were analyzed by two-tailed Mann-Whitney plotted with mean and SEM (n = 3 embryos per condition for each condition; representative of 3 independent experiments); ns: non-significant, *p < 0.05, **p < 0.01.

Figure 10. Reactive oxygen species are required for axon degeneration induced by BDNF deprivation. A) DRG explants cultured in NGF or BDNF were either maintained in trophic media or withdrawn from trophic support with or without ROS scavenger N-acetyl-cysteine (NAC, 20 mM) for 24 hours before fixing, immunostaining for βIII-tubulin and imaged by epifluorescence microscopy (NGF scale bar = 1000 μm; BDNF scale bar = 500 μm). B) Quantification of axonal area as a function of the distance from the soma and plotted in 500-μm bins segments relative to 0-500 μm 48-hour time point. NAC rescued degeneration induced by NGF deprivation and BDNF deprivation. The relative axonal area was analyzed by two-factor ANOVA followed by Tukey's *post hoc* comparison and plotted with mean and SEM (n = 3 embryos for each condition; data shown is representative of 3 independent experiments); (∗) ctr. versus dep. 24h; (#) dep. 24h versus dep. 24h + NAC; **p < 0.01, ****p < 0.0001.

References

Acheson A, Barker Pa, Alderson Rf, Miller Fd and Murphy Ra (1991) Detection of brain-derived neurotrophic factor-like activity in fibroblasts and Schwann cells: inhibition by antibodies to NGF. *Neuron,* 7, 265-75.

Bamji Sx, Majdan M, Pozniak Cd, Belliveau Dj, Aloyz R, Kohn J, Causing Cg and Miller Fd (1998) The p75 neurotrophin receptor mediates neuronal apoptosis and is essential for naturally occurring sympathetic neuron death. *J Cell Biol,* 140, 911-23.

Barde Ya (1989) Trophic factors and neuronal survival. *Neuron,* 2, 1525-34.

Barker Pa and Shooter Em (1994) Disruption of NGF binding to the low affinity neurotrophin receptor p75LNTR reduces NGF binding to TrkA on PC12 cells. *Neuron,* 13, 203-15.

Borasio Gd, John J, Wittinghofer A, Barde Ya, Sendtner M and Heumann R (1989) ras p21 protein promotes survival and fiber outgrowth of cultured embryonic neurons. *Neuron,* 2, 1087-96.

Burek Mj and Oppenheim Rw (1996) Programmed cell death in the developing nervous system. *Brain Pathol,* 6, 427-46.

Buss Rr, Sun W and Oppenheim Rw (2006) Adaptive roles of programmed cell death during nervous system development. *Annu Rev Neurosci,* 29, 1-35.

Carter Bd, Zirrgiebel U and Barde Ya (1995) Differential regulation of p21ras activation in neurons by nerve growth factor and brain-derived neurotrophic factor. *J Biol Chem,* 270, 21751-7.

Chang Lk and Johnson Em, Jr. (2002) Cyclosporin A inhibits caspase-independent death of NGF-deprived sympathetic neurons: a potential role for mitochondrial permeability transition. *J Cell Biol,* 157, 771-81.

Chang Lk, Schmidt Re and Johnson Em, Jr. (2003) Alternating metabolic pathways in NGF-deprived sympathetic neurons affect caspase-independent death. *J Cell Biol,* 162, 245-56.

Deppmann Cd, Mihalas S, Sharma N, Lonze Be, Niebur E and Ginty Dd (2008) A model for neuronal competition during development. *Science,* 320, 369-73.

689 Deshmukh M, Kuida K and Johnson Em, Jr. (2000) Caspase inhibition extends the
690 commitment to neuronal death beyond cytochrome c release to the point of
691 mitochondrial depolarization. *J Cell Biol,* 150, 131-43.
692 Ernfors P, Lee Kf and Jaenisch R (1994a) Mice lacking brain-derived neurotrophic
693 factor develop with sensory deficits. *Nature,* 368, 147-50.
694 Ernfors P, Lee Kf, Kucera J and Jaenisch R (1994b) Lack of neurotrophin-3 leads to
695 deficiencies in the peripheral nervous system and loss of limb proprioceptive
696 afferents. *Cell,* 77, 503-12.
697 Ernsberger U (2009) Role of neurotrophin signalling in the differentiation of neurons
698 from dorsal root ganglia and sympathetic ganglia. *Cell Tissue Res,* 336, 349-84.
699 Fariñas I, Wilkinson Ga, Backus C, Reichardt Lf and Patapoutian A (1998)
700 Characterization of neurotrophin and Trk receptor functions in developing
701 sensory ganglia: direct NT-3 activation of TrkB neurons in vivo. *Neuron,* 21, 325-
702 34.
703 Feinberg K, Kolaj A, Wu C, Grinshtein N, Krieger Jr, Moran Mf, Rubin Ll, Miller Fd and
704 Kaplan Dr (2017) A neuroprotective agent that inactivates prodegenerative TrkA
705 and preserves mitochondria. *J Cell Biol,* 216, 3655-3675.
706 Fischer Lr and Glass Jd (2007) Axonal degeneration in motor neuron disease.
707 *Neurodegener Dis,* 4, 431-42.
708 Fricker M, Tolkovsky Am, Borutaite V, Coleman M and Brown Gc (2018) Neuronal Cell
709 Death. *Physiol Rev,* 98, 813-880.
710 Garcia-Perez C, Roy Ss, Naghdi S, Lin X, Davies E and Hajnóczky G (2012) Bid-
711 induced mitochondrial membrane permeabilization waves propagated by local
712 reactive oxygen species (ROS) signaling. *Proc Natl Acad Sci U S A,* 109, 4497-
713 502.
714 Geden Mj, Romero Se and Deshmukh M (2019) Apoptosis versus axon pruning:
715 Molecular intersection of two distinct pathways for axon degeneration. *Neurosci*
716 *Res,* 139, 3-8.
717 Glebova No and Ginty Dd (2005) Growth and survival signals controlling sympathetic
718 nervous system development. *Annu Rev Neurosci,* 28, 191-222.

719 Haapasalo A, Sipola I, Larsson K, Akerman Ke, Stoilov P, Stamm S, Wong G and
720 Castren E (2002) Regulation of TRKB surface expression by brain-derived
721 neurotrophic factor and truncated TRKB isoforms. *J Biol Chem,* 277, 43160-7.
722 Hellard D, Brosenitsch T, Fritzsch B and Katz Dm (2004) Cranial sensory neuron
723 development in the absence of brain-derived neurotrophic factor in BDNF/Bax
724 double null mice. *Dev Biol,* 275, 34-43.
725 Huber K, Kuehnel F, Wyatt S and Davies Am (2000) TrkB expression and early sensory
726 neuron survival are independent of endogenous BDNF. *J Neurosci Res,* 59, 372-
727 8.
728 Jiang J, Huang Z, Zhao Q, Feng W, Belikova Na and Kagan Ve (2008) Interplay
729 between bax, reactive oxygen species production, and cardiolipin oxidation
730 during apoptosis. *Biochem Biophys Res Commun,* 368, 145-50.
731 Johnson Je, Barde Ya, Schwab M and Thoenen H (1986) Brain-derived neurotrophic
732 factor supports the survival of cultured rat retinal ganglion cells. *J Neurosci,* 6,
733 3031-8.
734 Johnstone Ad, De Léon A, Unsain N, Gibon J and Barker Pa (2019) Developmental
735 Axon Degeneration Requires TRPV1-Dependent Ca(2+) Influx. *eNeuro,* 6.
736 Johnstone Ad, Hallett Rm, De Léon A, Carturan B, Gibon J and Barker Pa (2018) A
737 novel method for quantifying axon degeneration. *PLoS One,* 13, e0199570.
738 Kalcheim C, Barde Ya, Thoenen H and Le Douarin Nm (1987) In vivo effect of brain-
739 derived neurotrophic factor on the survival of developing dorsal root ganglion
740 cells. *EMBO J,* 6, 2871-3.
741 Kalkavan H and Green Dr (2018) MOMP, cell suicide as a BCL-2 family business. *Cell
742 Death Differ,* 25, 46-55.
743 Kanaan Nm, Pigino Gf, Brady St, Lazarov O, Binder Li and Morfini Ga (2013) Axonal
744 degeneration in Alzheimer's disease: when signaling abnormalities meet the
745 axonal transport system. *Exp Neurol,* 246, 44-53.
746 Kirkland Ra and Franklin Jl (2001) Evidence for redox regulation of cytochrome C
747 release during programmed neuronal death: antioxidant effects of protein
748 synthesis and caspase inhibition. *J Neurosci,* 21, 1949-63.

749 Kirkland Ra and Franklin Jl (2003) Bax, reactive oxygen, and cytochrome c release in
750 neuronal apoptosis. *Antioxid Redox Signal,* 5, 589-96.
751 Kirkland Ra and Franklin Jl (2007) Bax affects production of reactive oxygen by the
752 mitochondria of non-apoptotic neurons. *Exp Neurol,* 204, 458-61.
753 Kirkland Ra, Saavedra Gm, Cummings Bs and Franklin Jl (2010) Bax regulates
754 production of superoxide in both apoptotic and nonapoptotic neurons: role of
755 caspases. *J Neurosci,* 30, 16114-27.
756 Kirkland Ra, Windelborn Ja, Kasprzak Jm and Franklin Jl (2002) A Bax-induced pro-
757 oxidant state is critical for cytochrome c release during programmed neuronal
758 death. *J Neurosci,* 22, 6480-90.
759 Kirstein M and Fariñas I (2002) Sensing life: regulation of sensory neuron survival by
760 neurotrophins. *Cell Mol Life Sci,* 59, 1787-802.
761 Knudson Cm, Tung Ks, Tourtellotte Wg, Brown Ga and Korsmeyer Sj (1995) Bax-
762 deficient mice with lymphoid hyperplasia and male germ cell death. *Science,* 270,
763 96-9.
764 Lallemend F and Ernfors P (2012) Molecular interactions underlying the specification of
765 sensory neurons. *Trends Neurosci,* 35, 373-81.
766 Lamarche F, Carcenac C, Gonthier B, Cottet-Rousselle C, Chauvin C, Barret L, Leverve
767 X, Savasta M and Fontaine E (2013) Mitochondrial permeability transition pore
768 inhibitors prevent ethanol-induced neuronal death in mice. *Chem Res Toxicol,*
769 26, 78-88.
770 Lang-Rollin Ic, Rideout Hj, Noticewala M and Stefanis L (2003) Mechanisms of
771 caspase-independent neuronal death: energy depletion and free radical
772 generation. *J Neurosci,* 23, 11015-25.
773 Lee Kf, Li E, Huber Lj, Landis Sc, Sharpe Ah, Chao Mv and Jaenisch R (1992) Targeted
774 mutation of the gene encoding the low affinity NGF receptor p75 leads to deficits
775 in the peripheral sensory nervous system. *Cell,* 69, 737-49.
776 Levi-Montalcini R and Booker B (1960) DESTRUCTION OF THE SYMPATHETIC
777 GANGLIA IN MAMMALS BY AN ANTISERUM TO A NERVE-GROWTH
778 PROTEIN. *Proc Natl Acad Sci U S A,* 46, 384-91.

779 Liebl Dj, Tessarollo L, Palko Me and Parada Lf (1997) Absence of sensory neurons
780 before target innervation in brain-derived neurotrophic factor-, neurotrophin 3-,
781 and TrkC-deficient embryonic mice. *J Neurosci,* 17, 9113-21.
782 Mehlen P and Bredesen De (2004) The dependence receptor hypothesis. *Apoptosis,* 9,
783 37-49.
784 Nikoletopoulou V, Lickert H, Frade Jm, Rencurel C, Giallonardo P, Zhang L, Bibel M
785 and Barde Ya (2010) Neurotrophin receptors TrkA and TrkC cause neuronal
786 death whereas TrkB does not. *Nature,* 467, 59-63.
787 Patel Td, Jackman A, Rice Fl, Kucera J and Snider Wd (2000) Development of sensory
788 neurons in the absence of NGF/TrkA signaling in vivo. *Neuron,* 25, 345-57.
789 Roux Pp and Barker Pa (2002) Neurotrophin signaling through the p75 neurotrophin
790 receptor. *Prog Neurobiol,* 67, 203-33.
791 Saxena S and Caroni P (2007) Mechanisms of axon degeneration: from development to
792 disease. *Prog Neurobiol,* 83, 174-91.
793 Schoenmann Z, Assa-Kunik E, Tiomny S, Minis A, Haklai-Topper L, Arama E and Yaron
794 A (2010) Axonal degeneration is regulated by the apoptotic machinery or a
795 NAD+-sensitive pathway in insects and mammals. *J Neurosci,* 30, 6375-86.
796 Schuldiner O and Yaron A (2015) Mechanisms of developmental neurite pruning. *Cell*
797 *Mol Life Sci,* 72, 101-19.
798 Shacham-Silverberg V, Sar Shalom H, Goldner R, Golan-Vaishenker Y, Gurwicz N,
799 Gokhman I and Yaron A (2018) Phosphatidylserine is a marker for axonal debris
800 engulfment but its exposure can be decoupled from degeneration. *Cell Death*
801 *Dis,* 9, 1116.
802 Simon Dj, Weimer Rm, Mclaughlin T, Kallop D, Stanger K, Yang J, O'leary Dd,
803 Hannoush Rn and Tessier-Lavigne M (2012) A caspase cascade regulating
804 developmental axon degeneration. *J Neurosci,* 32, 17540-53.
805 Singh Kk, Park Kj, Hong Ej, Kramer Bm, Greenberg Me, Kaplan Dr and Miller Fd (2008)
806 Developmental axon pruning mediated by BDNF-p75NTR-dependent axon
807 degeneration. *Nat Neurosci,* 11, 649-58.
808 Sommerfeld Mt, Schweigreiter R, Barde Ya and Hoppe E (2000) Down-regulation of the
809 neurotrophin receptor TrkB following ligand binding. Evidence for an involvement

of the proteasome and differential regulation of TrkA and TrkB. *J Biol Chem,* 275, 8982-90.

Tait Sw and Green Dr (2010) Mitochondria and cell death: outer membrane permeabilization and beyond. *Nat Rev Mol Cell Biol,* 11, 621-32.

Tauszig-Delamasure S, Yu Ly, Cabrera Jr, Bouzas-Rodriguez J, Mermet-Bouvier C, Guix C, Bordeaux Mc, Arumäe U and Mehlen P (2007) The TrkC receptor induces apoptosis when the dependence receptor notion meets the neurotrophin paradigm. *Proc Natl Acad Sci U S A,* 104, 13361-6.

Tessarollo L, Tsoulfas P, Donovan Mj, Palko Me, Blair-Flynn J, Hempstead Bl and Parada Lf (1997) Targeted deletion of all isoforms of the trkC gene suggests the use of alternate receptors by its ligand neurotrophin-3 in neuronal development and implicates trkC in normal cardiogenesis. *Proc Natl Acad Sci U S A,* 94, 14776-81.

Unsain N, Heard Kn, Higgins Jm and Barker Pa (2014) Production and isolation of axons from sensory neurons for biochemical analysis using porous filters. *J Vis Exp*.

Unsain N, Higgins Jm, Parker Kn, Johnstone Ad and Barker Pa (2013) XIAP regulates caspase activity in degenerating axons. *Cell Rep,* 4, 751-63.

Valdés-Sánchez T, Kirstein M, Pérez-Villalba A, Vega Ja and Fariñas I (2010) BDNF is essentially required for the early postnatal survival of nociceptors. *Dev Biol,* 339, 465-76.

Vickers Jc, King Ae, Woodhouse A, Kirkcaldie Mt, Staal Ja, Mccormack Gh, Blizzard Ca, Musgrove Re, Mitew S, Liu Y, Chuckowree Ja, Bibari O and Dickson Tc (2009) Axonopathy and cytoskeletal disruption in degenerative diseases of the central nervous system. *Brain Res Bull,* 80, 217-23.

Wakatsuki S and Araki T (2017) Specific phospholipid scramblases are involved in exposure of phosphatidylserine, an "eat-me" signal for phagocytes, on degenerating axons. *Commun Integr Biol,* 10, e1296615.

Wilson C, Muñoz-Palma E and González-Billault C (2018) From birth to death: A role for reactive oxygen species in neuronal development. *Semin Cell Dev Biol,* 80, 43-49.

Figure 1

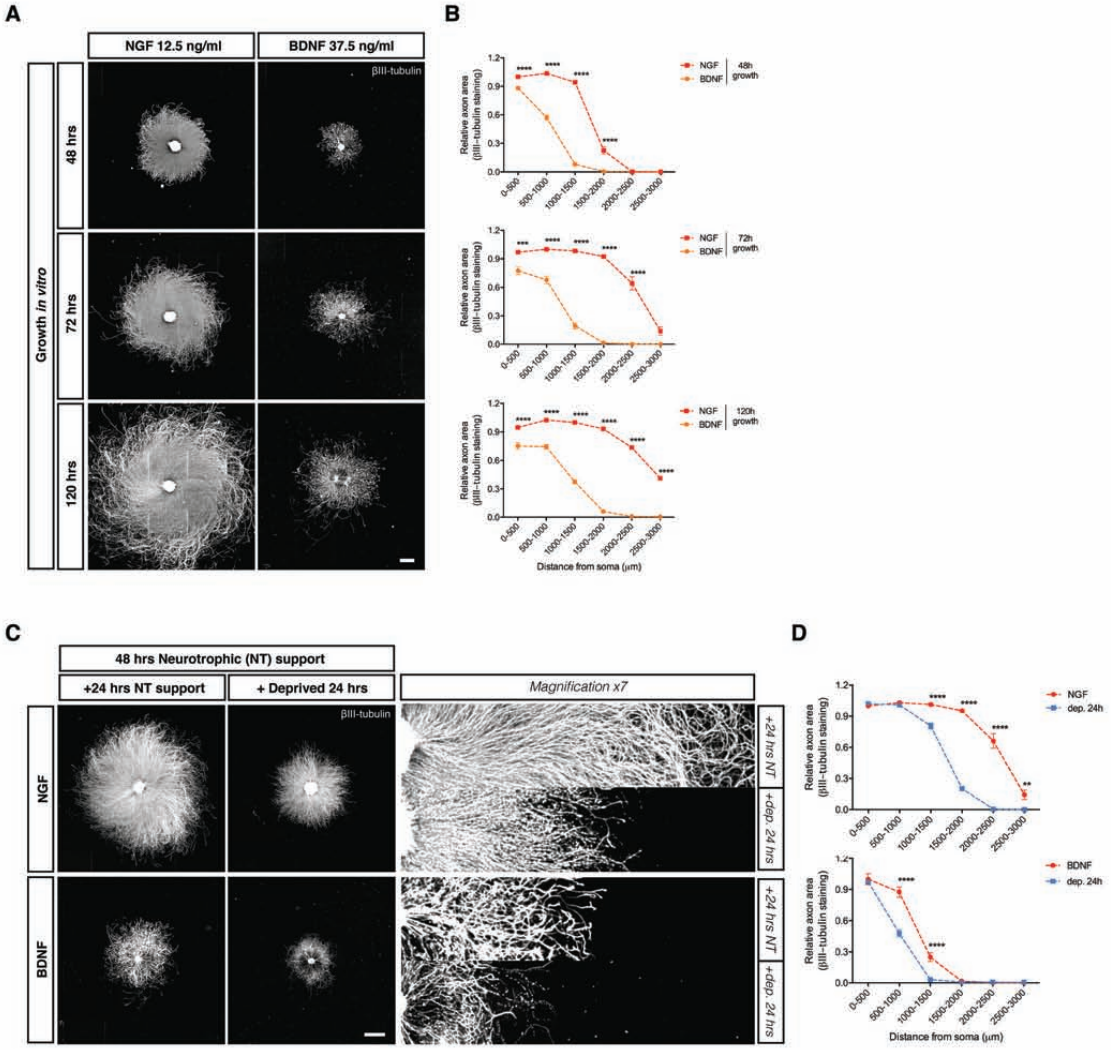

Figure 2

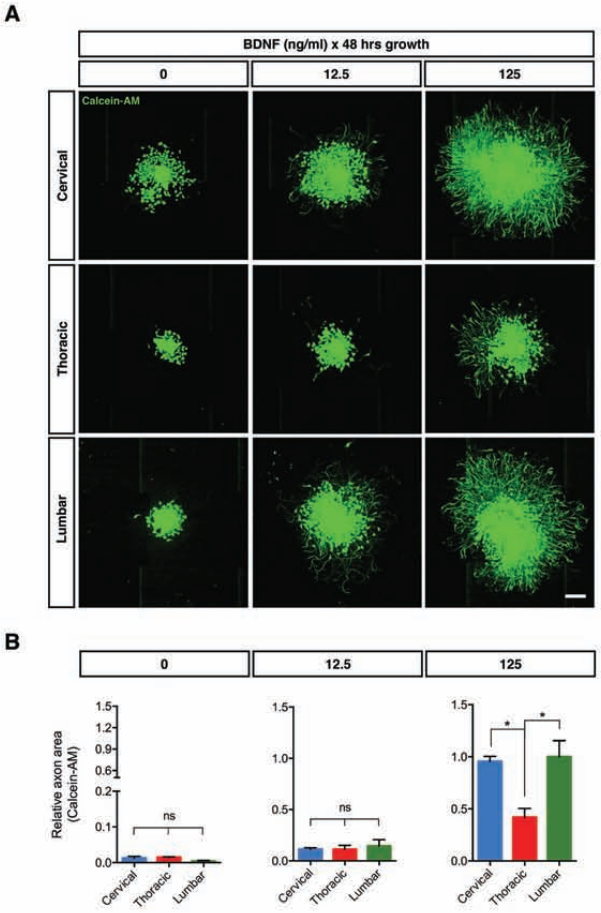

Figure 3

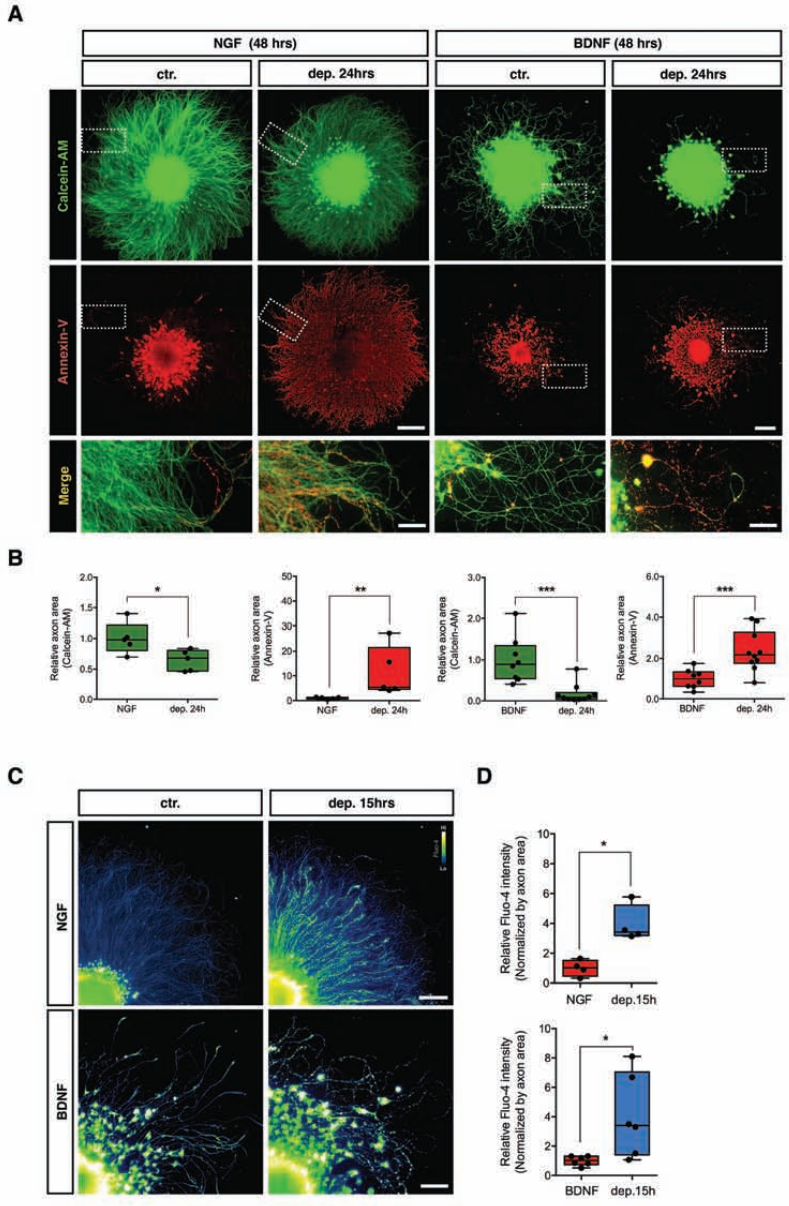

Figure 4

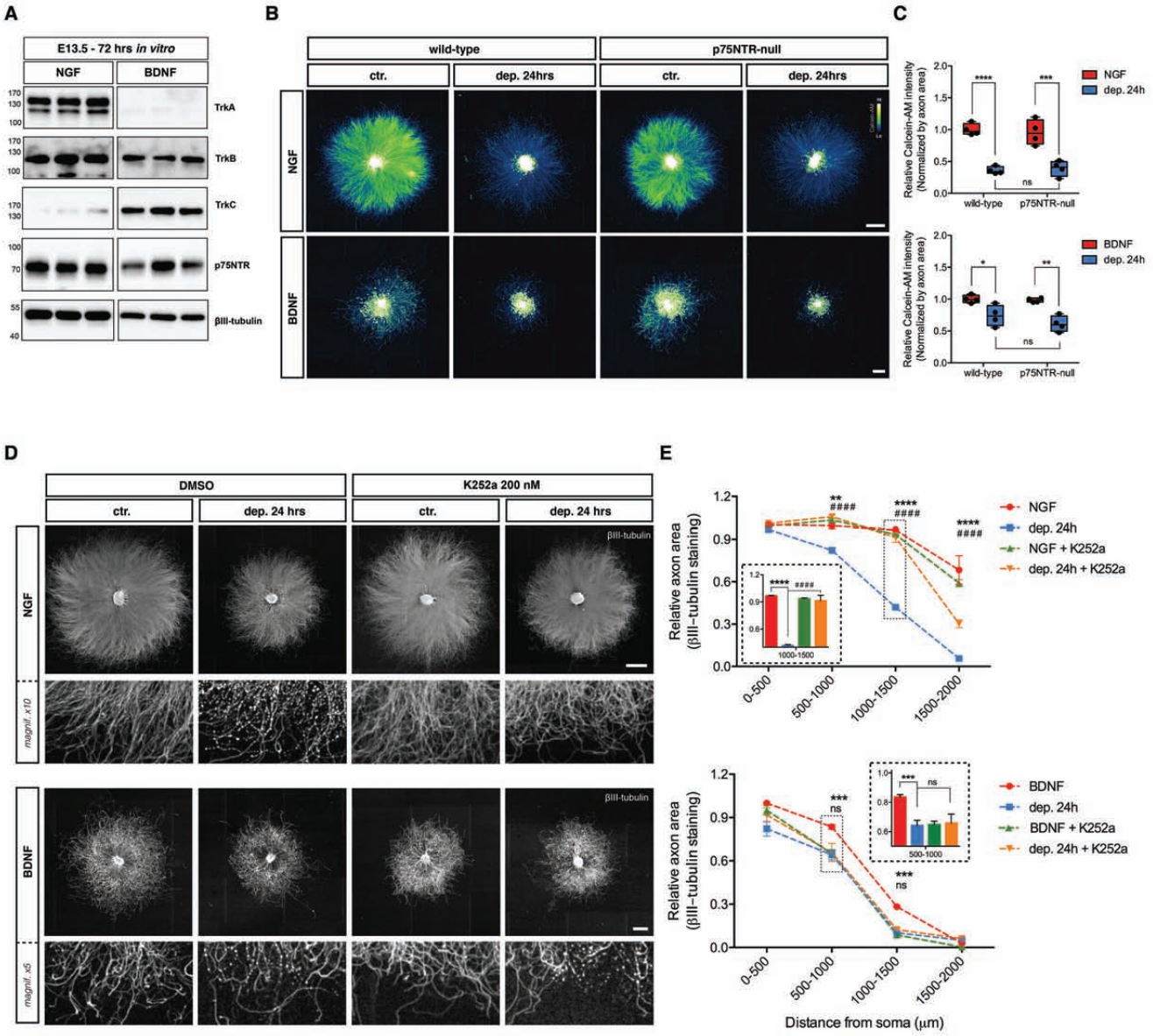

Figure 5

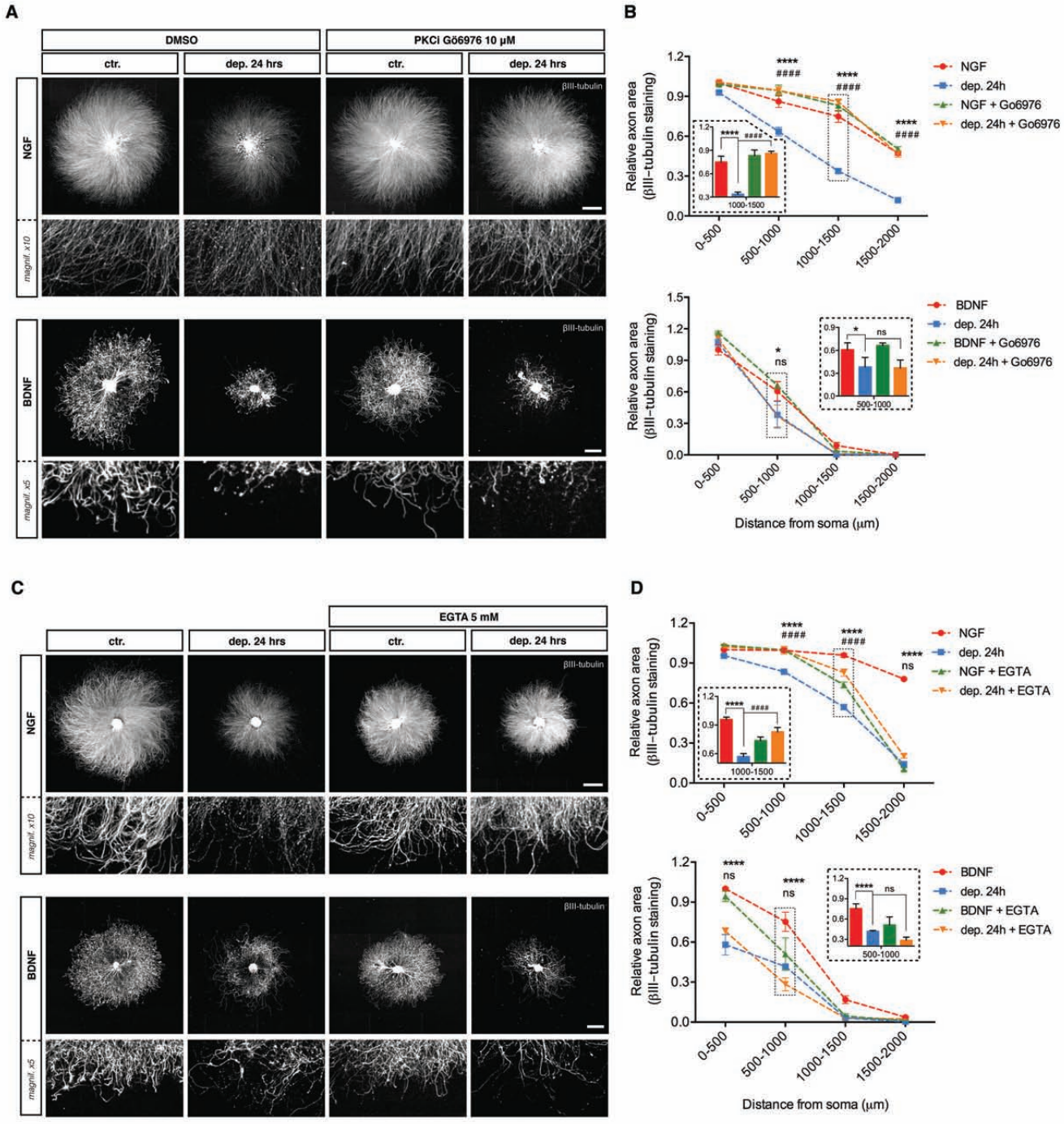

Figure 6 cont.

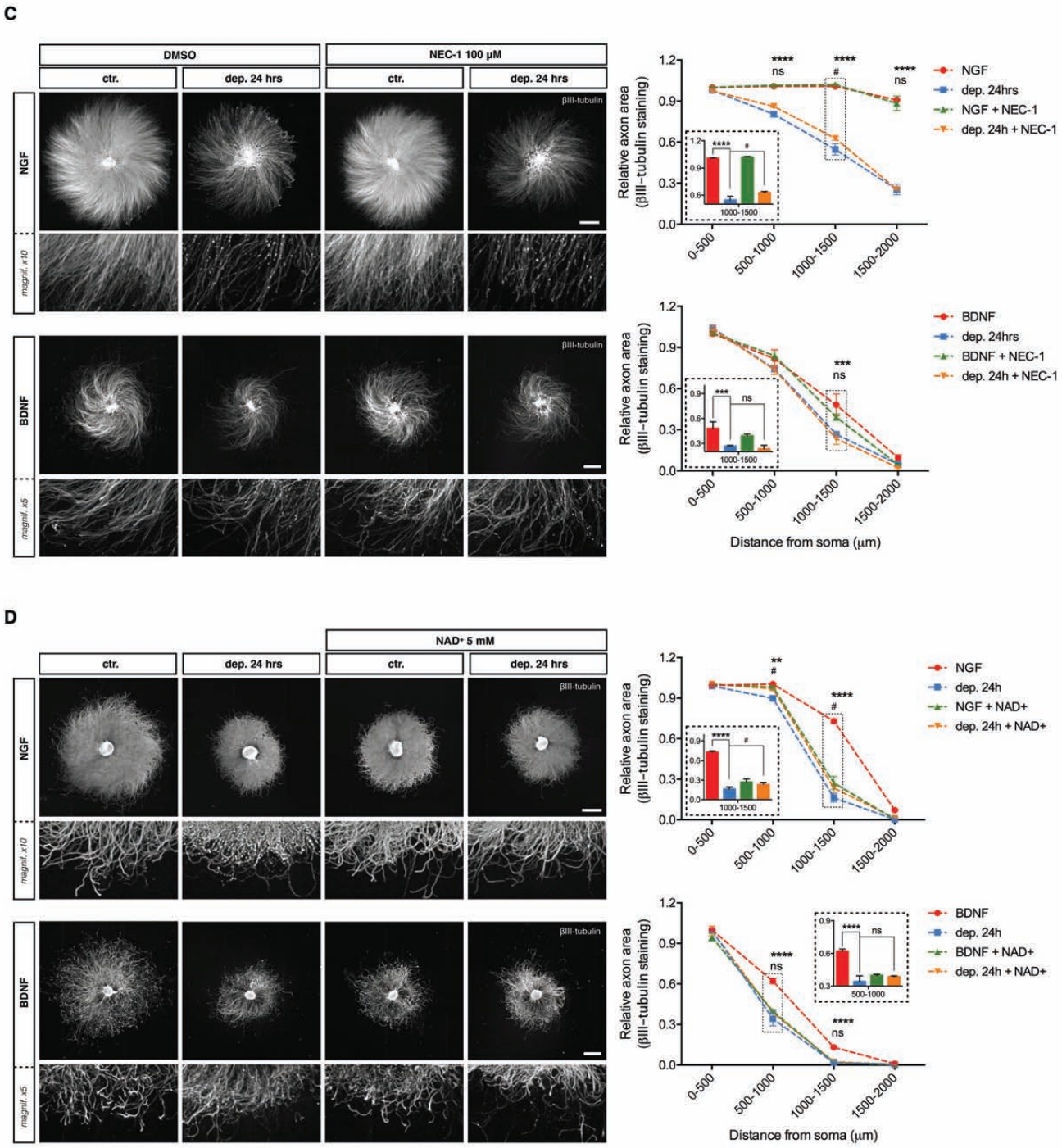

Figure 7

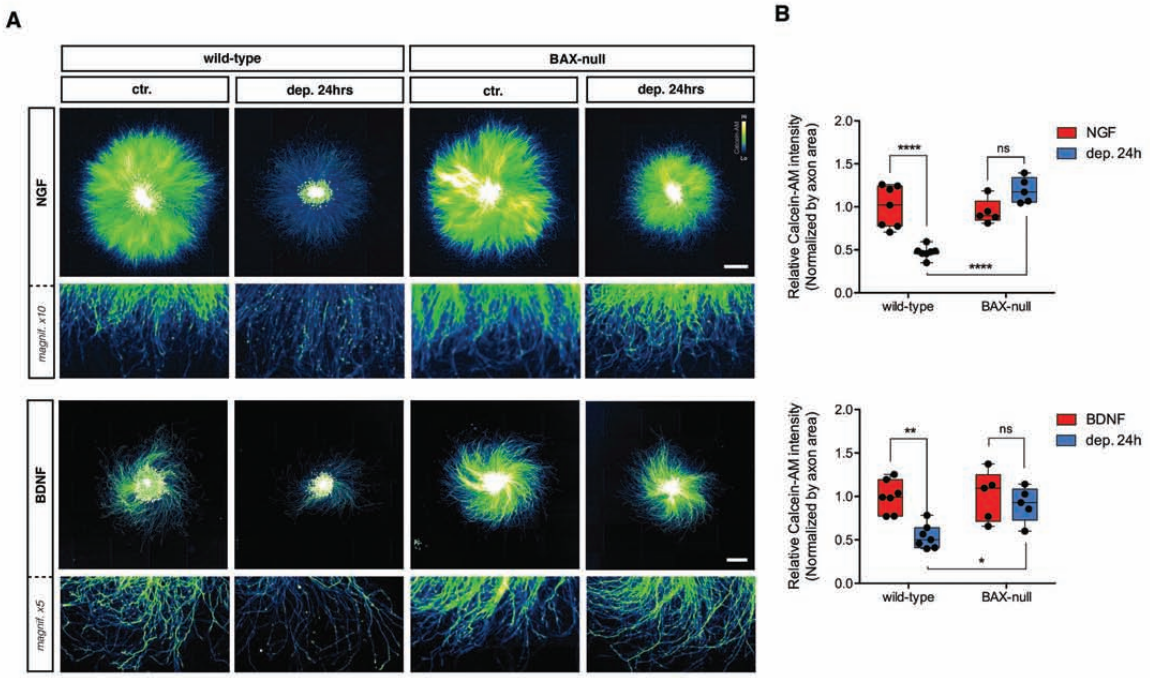

Figure 8

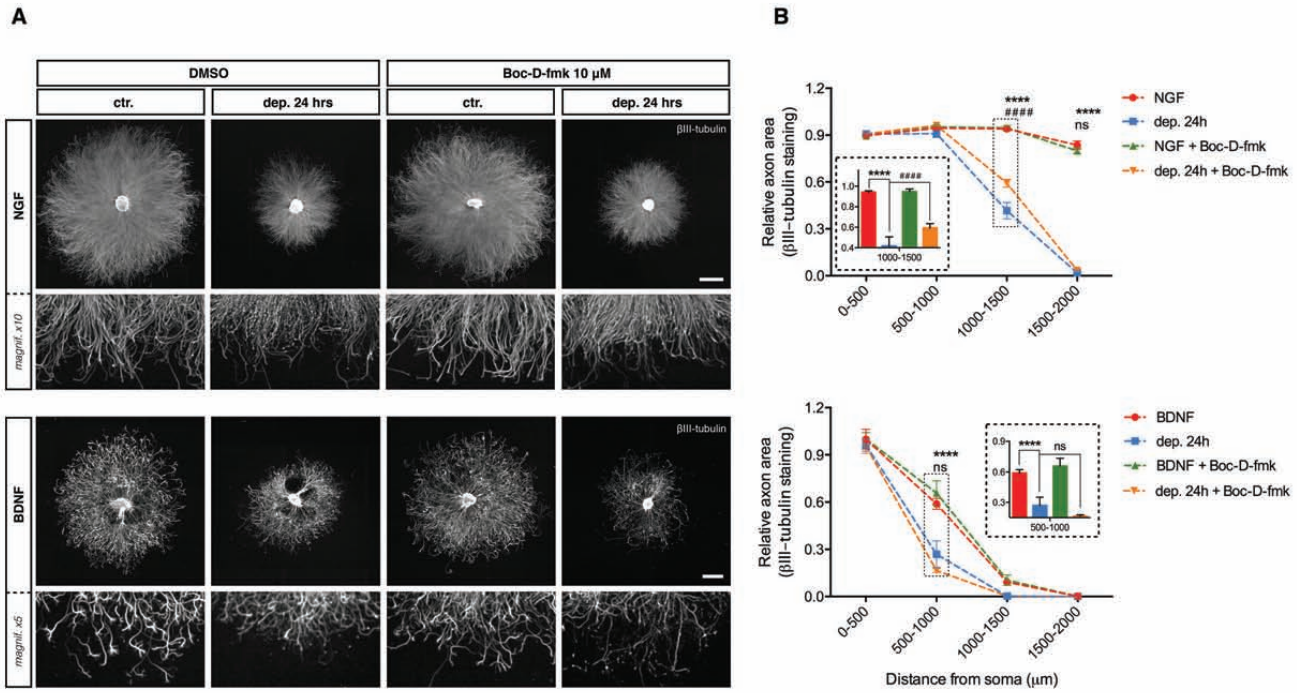

Figure 9

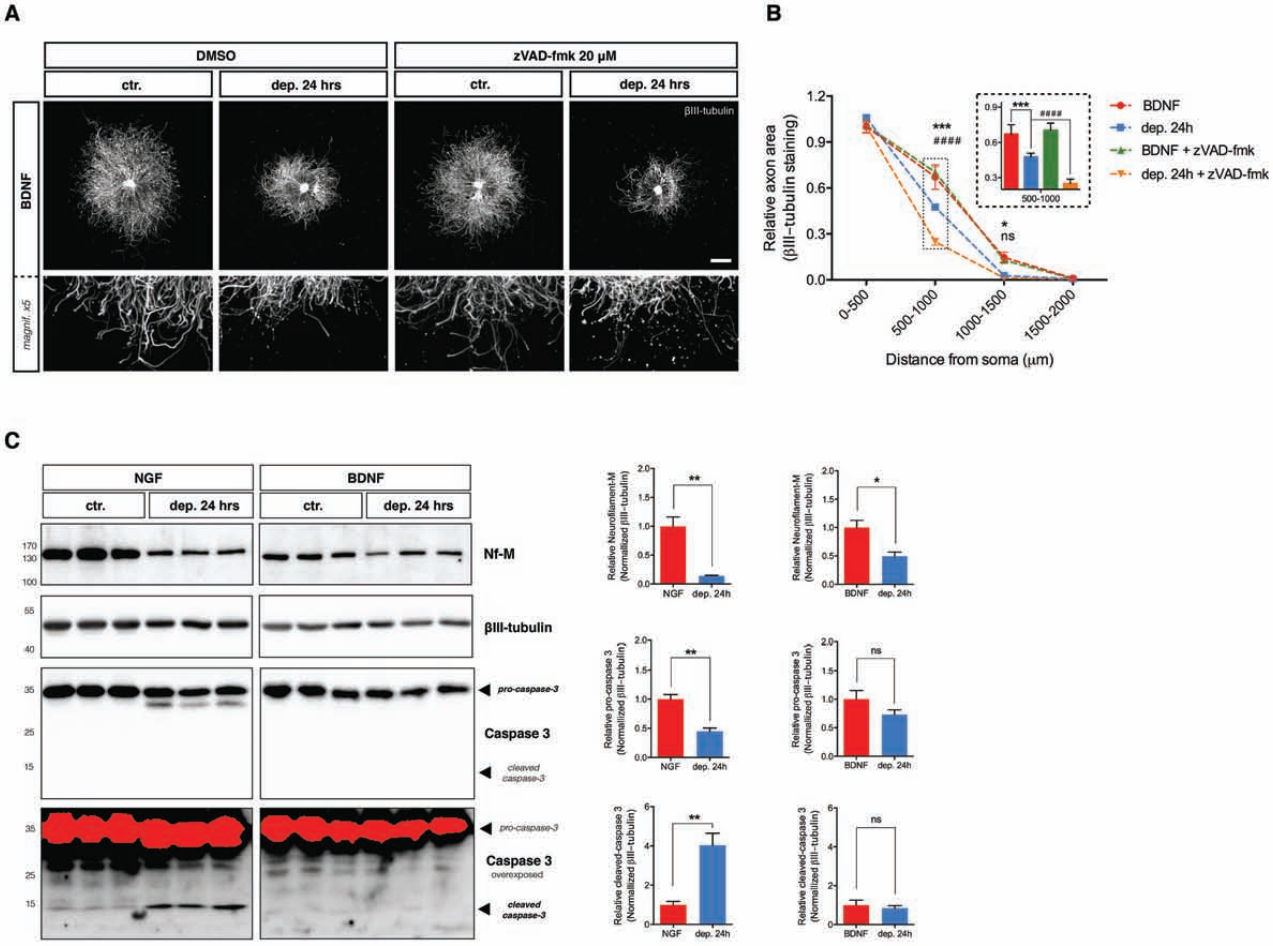

Figure 10